THE OFFICIAL MAGAZINE OF THE OCEANOGRAPHY SOCIETY

Oceanography

CITATION

Dong, S., G. Goni, and R. Lumpkin. 2015. Mixed-layer salinity budget in the SPURS region on seasonal to interannual time scales. *Oceanography* 28(1):78–85, http://dx.doi.org/10.5670/oceanog.2015.05.

DOI

http://dx.doi.org/10.5670/oceanog.2015.05

Mixed-Layer Salinity Budget

in the SPURS Region on Seasonal to Interannual Time Scales

By Shenfu Dong, Gustavo Goni, and Rick Lumpkin

ABSTRACT. Surface salinity variations and processes affecting surface salinity in the high-salinity region of the subtropical North Atlantic (the SPURS-1 area) are investigated by combining data from in situ observations and satellite remote-sensing measurements. On temporal average, the surface freshwater flux term (evaporation minus precipitation) in the SPURS-1 region increases mixed-layer salinity. Oceanic advection plays the largest role in compensating this salinity increase. On seasonal time scales, mixed-layer salinity increases from April to August and decreases from September to March. This seasonal evolution of the mixed-layer salinity is largely controlled by the freshwater flux term, with vertical entrainment playing a secondary role. The domain-averaged oceanic advection and diffusion terms do not show significant seasonal cycles. The sum of all estimated salinity budget terms largely captures salinity variations on interannual time scales. Unlike the seasonal cycle, variations in freshwater flux, oceanic advection, and vertical entrainment all contribute to interannual variations in surface salinity. Oceanic advection plays a larger role in salinity changes during 2008–2012, whereas the surface freshwater flux term dominates surface salinity evolution during 2004–2007 and in 2013. Although evaporation in the SPURS-1 region dominates the mean freshwater flux, precipitation plays a larger role in interannual variations of the freshwater flux. Separating the advection term into geostrophic and Ekman components indicates that the Ekman component dominates the total advection term. The effect of Ekman advection on salinity changes in the SPURS-1 region is closely linked to the spatial distribution of salinity anomalies. Therefore, it is important to understand large-scale forcing changes.

INTRODUCTION

Temperature and salinity are the two fundamental ocean state variables. In contrast to extensive studies of ocean temperature, ocean salinity has received much less attention, mainly due to lack of data, but also because ocean salinity is generally perceived to have no direct influence on ocean-atmosphere interaction. However, through modification of oceanic density fields, salinity can impact ocean circulation and mixing (e.g., Fedorov et al., 2004; Huang et al., 2005), which in turn affects ocean temperature. Thus, salinity can play a substantial role in ocean-atmosphere interaction and the global climate system, particularly at lower latitudes where the existence of a barrier layer, defined as the layer between the bottom of a shallow halocline and the top of the thermocline, has been observed (Lukas and Lindstrom, 1991; Sprintall and Tomczak, 1992; Godfrey et al., 1999) and at high latitudes where salinity dominates thermohaline circulation (de Boyer Montegut et al., 2007). Formation and erosion of the barrier layer greatly influences surface mixed-layer dynamics. It impacts entrainment of cooler thermocline waters into the surface mixed layer, and thus regulates heat and momentum exchanges between the ocean and the atmosphere.

The ocean also acts as a salt reservoir, whose salt content is conserved over time. Thus, the distribution of ocean salinity can be used to estimate freshwater flux (e.g., evaporation and precipitation) and transport as well as ocean mixing processes (Lukas and Lindstrom, 1991). Ocean salinity can also be used as an indicator of the strength of the water cycle. Durack and Wijffels (2010) assembled all available salinity data for the period 1950–2000 and found a sea surface salinity increase in evaporation-dominated regions and a decrease in precipitation-dominated regions. The resemblance of the spatial pattern of salinity change to the mean salinity field suggests an amplification of the global water cycle (i.e., strengthening of the processes responsible for mean surface salinity distribution; Schmitt, 2008; Durack et al., 2012). This resemblance also indicates that changes in ocean salinity are more robust indicators of global water cycle changes than estimated changes in evaporation minus precipitation (E–P). During recent decades, large-scale changes of salinity have been observed in certain regions. A number of studies have described freshening at high latitudes (e.g., Wong et al., 1999; Bindoff and McDougall, 2000; Curry et al., 2003; Curry and Mauritzen, 2005; Josey and Marsh, 2005), while Curry et al. (2003) found a systematic increase in salinity at low latitudes of the North Atlantic Ocean. However, these changes have not been explained. Understanding the physical processes governing these

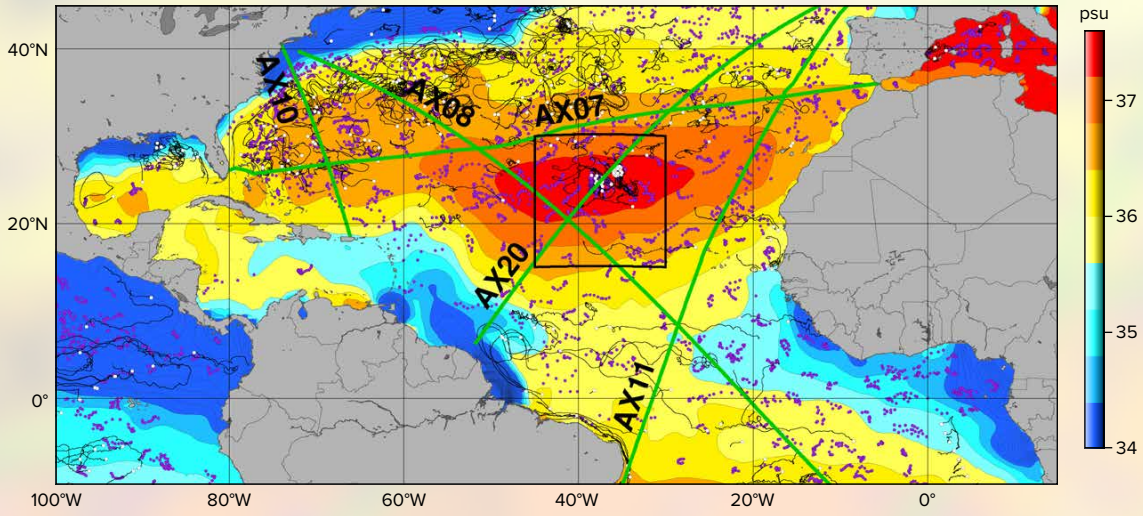

Figure 1. Mean sea surface salinity from the World Ocean Atlas 2009 (color shading). The black box indicates the SPURS-1 region. Green lines correspond to the locations of major repeated expendable bathythermograph (XBT) transects. The locations of Argo profiling floats and surface drifter trajectories during August–October 2012, corresponding to the September 2012 SPURS-1 cruise, are shown as magenta dots and black lines, respectively.

salinity changes is particularly important to advance our understanding of the global water cycle.

In recent years, much attention has been paid to the Atlantic Meridional Overturning Circulation (AMOC) because of its potential links to past abrupt climate changes and anthropogenic climate forcing (e.g., Broecker, 1997; Stocker and Schmittner, 1997; Gregory et al., 2005). Sea surface salinity (SSS) at high latitudes is thought to influence AMOC intensity through its effect on the formation of North Atlantic Deep Water (e.g., Rahmstorf, 1995; Häkkinen, 1999). AMOC strength controls oceanic uptake of carbon dioxide in the North Atlantic, suggesting that salinity may be influential in determining future climate.

Despite the importance of salinity to the global water cycle and climate system, our understanding of the physical processes and feedbacks involving salinity changes remains limited, in large part due to the lack of observations. Although the time-mean distribution of sea surface salinity is related to net freshwater flux (E–P), with high salinities in the evaporative subtropics and reduced salinities in the tropics and subpolar regions where there is high precipitation, the regions with high/low salinities and positive/negative freshwater fluxes are not well collocated. For example, the subtropical salinity maxima generally occur on the poleward side of high evaporation regions. Although this displacement has been attributed to poleward Ekman advection of high salinity water in the subtropics (O'Connor et al., 2005), a recent study (Qu et al., 2013) suggests that the North Atlantic salinity maximum water comes from the northwestern part of the subtropical gyre. Clearly, the roles that different physical processes play in forming and dissipating salinity maxima and minima have not been well investigated and are not fully understood.

Many studies have examined seasonal variations in SSS (Boyer and Levitus, 2002; Yu, 2011; Bingham et al., 2012), particularly in the tropics (e.g., Bingham and Lukas, 1996; Johnson et al., 2002; Foltz and McPhaden, 2008). The dominant forcing for SSS seasonal variations differs regionally, with freshwater flux dominating in the tropical convergence zones and Ekman advection dominating in the subtropics. In contrast, SSS budgets on interannual to longer time scales have not been well studied due to the limitation of available observations. More recently, Vinogradova and Ponte (2013) and Qu et al. (2011, 2013) examined SSS budgets on interannual time scales using results from the Consortium for Estimating the Circulation and Climate of the Ocean (ECCO) model. Both freshwater flux and oceanic processes were found to contribute to salinity changes, demonstrating the important role the ocean plays in surface salinity changes. Observational-based salinity budgets on interannual to longer time scales have been difficult to calculate due to uncertainties in various data sets.

In order to characterize and predict changes in the global water cycle and global climate system, it is critical to advance our knowledge of the processes controlling ocean salinity variability. Improving the salinity monitoring system is essential for identifying changes in ocean salinity and understanding the physical processes responsible for those changes. A dedicated research effort, Salinity Processes in the Upper-ocean Regional Study (SPURS), explored the salinity maximum region in the North Atlantic Ocean (SPURS-1). The program included a series of cruises during the period September 2012 to October 2013 to collect in situ data (Figure 1). The dedicated observational and modeling effort of the SPURS-1 program and the synthesis of the SPURS-1 field observations will greatly improve our understanding of the governing processes and our ability to model the upper-ocean salinity evolution in the subtropical North Atlantic. With

the synthesis program focused on the short SPURS-1 period and the observed strong long-term variability of the salinity in the region, there is a need for an analysis of the salinity changes in the SPURS-1 region on interannual to longer time scales. In this study, we investigate interannual surface salinity variations and processes affecting surface salinity in the SPURS-1 region (15°N–30°N, 45°W–30°W) with a focus on the 10-year period 2004–2013. This interannual analysis sheds light on how upper-ocean conditions during the SPURS-1 period compared against the historical record provided by sustained ocean observing systems, including Argo profiling floats, surface drifters, and expendable bathythermograph (XBT) transects (Figure 1). Our analysis relies primarily on satellite measurements of sea surface height, ocean surface winds, precipitation, and in situ observations from Argo profiling floats, XBTs, and surface drifters. This analysis tests how well the mixed-layer salinity budget can be closed on various time scales with currently available observations.

We note that the observations from Argo floats, drifters, and XBTs are part of the large-scale component of the SPURS program. In support of SPURS-1, the National Oceanic and Atmospheric Administration's Atlantic Oceanographic and Meteorological Laboratory (NOAA/AOML) enhanced its observational networks by deploying additional XBTs on three transects, installing and maintaining a thermosalinograph (TSG) on a ship along the AX08 transect (Figure 1), and launching additional Argo floats and drifters in the SPURS-1 region.

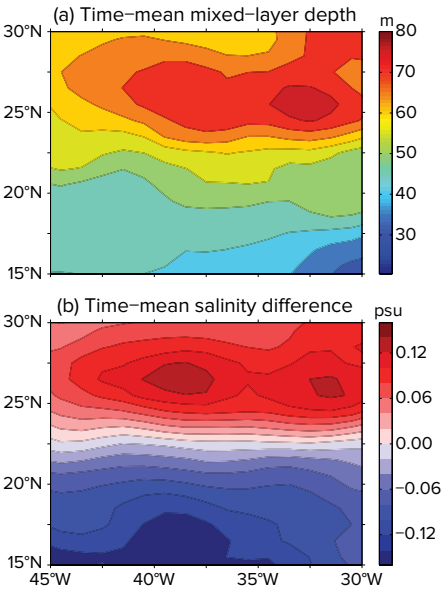

Figure 2. Time-mean (a) mixed-layer depth, and (b) salinity difference between the mixed layer and just below the mixed layer. Units are meters for the mixed-layer depth and psu (practical salinity units) for salinity differences.

DATA AND METHODOLOGY

Salinity changes in the surface mixed layer can be approximated by the sum of the surface freshwater flux term, horizontal advection, vertical entrainment, eddy diffusion, and mixing processes (e.g., Dong et al., 2009). The role of these processes in the observed mixed-layer salinity changes are estimated using data sets available from in situ and satellite measurements. The gridded temperature/salinity monthly fields from Argo floats for the period 2004–2013 (Roemmich and Gilson, 2009) are used to examine mixed-layer salinity changes ($\partial S_m/\partial t$). Those 1° × 1° gridded maps are also used to compute the mixed-layer depth (h_m) based on a density-difference criterion, $\Delta\rho = 0.125$ kg m^{-3}, where $\Delta\rho$ is the density difference from the topmost near-surface value. This value is an appropriate choice for calculating mixed-layer depth from a climatology (de Boyer Montégut et al., 2004), as opposed to typically smaller density differences used when deriving mixed-layer depth from individual profiles. The spatial distribution of mixed-layer depth (Figure 2a) is similar to the surface salinity structure, with the maximum mixed-layer depth overlapping the salinity maximum region.

The freshwater flux term, $(E–P)S_m/h_m$, includes two components, evaporation (E) and precipitation (P), and a number of E and P products are available. Monthly precipitation from the Global Precipitation Climatology Project (GPCP; Adler et al., 2003) and evaporation from the Objectively Analyzed air-sea Fluxes (OAFlux; Yu and Weller, 2007) were used in this study because this combination provided the best balance in terms of root-mean-square (RMS) differences between the salinity tendency and the sum of the contributions from the freshwater flux, ocean advection-diffusion, and entrainment processes. The OAFlux product integrates satellite observations with surface moorings, ship reports, and atmospheric model reanalyzed outputs. The monthly OAFlux evaporation is available on a 1° × 1° grid. The GPCP precipitation is available on a 2.5° × 2.5° grid from 1979 to the present.

The oceanic advection term $(-u_m\cdot\nabla S_m)$ includes both the geostrophic $(-u_g\cdot\nabla S_m)$ and the Ekman $(-u_e\cdot\nabla S_m)$ components. The geostrophic velocity (u_g) product produced by AVISO (Archiving, Validation and Interpretation of Satellite Oceanographic data), which is derived from the merged sea surface height (SSH) fields of all available satellites (Topex/Poseidon, Jason-1, ERS-1 and -2, Envisat, and GFO), was used to compute the geostrophic advection. The satellite-derived geostrophic velocity fields have seven-day temporal resolution and 1/3° × 1/3° spatial resolution (Ducet et al., 2000). The monthly wind stress fields (τ) from the ERA-interim (Dee et al., 2011) were used to estimate the Ekman velocity,

$$u_e = \tau \times \vec{z} \,/\, \rho f h_m$$

with water density ρ and the Coriolis parameter f. The ERA-interim winds are provided on a 0.75° × 0.75° grid. To be consistent with the temporal period and the spatial resolution of the salinity data, the satellite velocity fields were averaged to produce a monthly climatology on a 1° × 1° grid.[1]

Entrainment of water from below the base of the mixed layer can also induce changes in mixed-layer salinity due to salinity differences (ΔS) between the mixed layer and just below the mixed

[1] ERA-Interim is a global atmospheric reanalysis from 1979, continuously updated in real time.

layer. For our investigation, the entrainment velocity (w_e) was approximated as the time rate of change of the mixed-layer depth ($\partial h_m/\partial t$). The entrainment velocity was set to zero during the detraining period. Salinity differences (ΔS) were calculated from the monthly Argo salinity fields, corresponding to the difference between mixed-layer salinity and salinity averaged in the 10 m water column below the mixed layer. The 10 m layer thickness is chosen based on the entrainment velocity, which gives a mean value of 10 m on average. These salinity differences are positive north of 23°N (Figure 2b), indicating that the mixed layer is saltier than the subsurface layer. South of 23°N, the mixed layer is fresher than the subsurface, as shown by the negative salinity differences. This suggests that the entrainment term ($-w_e\Delta S/h_m$) would decrease mixed-layer salinity north of 23°N, but increase mixed-layer salinity to the south.

We also compute the horizontal diffusion term ($\kappa_h\nabla^2 S_m$) using salinity from Argo with the horizontal eddy diffusivity κ_h = 5,000 m^2 s^{-1}, as estimated from the SPURS-1 field program (Schmitt and Blair, 2015, in this issue).

MEAN STATE

All terms contributing to mixed-layer salinity changes are nearly balanced when averaged over the 10-year period and over the SPURS-1 region, with positive values of 0.82 ± 0.04 psu yr^{-1} for the freshwater flux term and negative values of −0.56 ± 0.03, −0.05 ± 0.02, and −0.28 ± 0.01 psu yr^{-1} for the oceanic advection, vertical entrainment, and horizontal diffusion terms, respectively. Although the total advection is negative, the geostrophic component is positive (0.17 ± 0.01 psu yr^{-1}), which partially compensates the freshening effect of the Ekman advection (−0.73 ± 0.03 psu yr^{-1}). The mean salinity tendency ($\partial S_m/\partial t$) is very small, −0.01 ± 0.06 psu yr^{-1}, not statistically different from zero. The residual ($\partial S_m/\partial t$ – sum of forcing terms) of 0.06 psu yr^{-1} is likely due to uncertainties in the data, because the unresolved mixing process tends to be negative (Qu et al., 2011).

The spatial distributions of the time-mean terms (Figure 3) show that the freshwater flux term is positive throughout the SPURS-1 region, varying between 0.54 and 1.07 psu yr^{-1}, with its maximum along 20°N. In contrast, the oceanic advection term is mostly negative, acting to decrease salinity in the region. The magnitude of the advection term decreases from the south to the north because both velocity and salinity gradients are stronger in the south. Dividing the advection term into Ekman and geostrophic components (Figure 3c,d) shows that the two components compensate each other. The Ekman advection term is positive north of 25°N, and the geostrophic advection term is negative with slightly larger magnitude, resulting in a negative total advection term. South of 25°N, the Ekman advection term is negative, and the geostrophic advection term is positive. Further dividing the advection into zonal and meridional components indicates that the meridional advection dominates both the Ekman and geostrophic advection terms owing to the relative strong meridional velocity and large meridional salinity gradient. The sign change of the advection terms north and south of 25°N is due to the change of sign in the meridional salinity gradient because of the maximum salinity along 25°N. Following the spatial distribution of the salinity differences (Figure 2b), the entrainment term is positive south of 23°N and negative to the north. As a result, the spatially averaged freshening effect from the entrainment is very small. The horizontal diffusion term is mostly negative, except in the regions close to the northern and southern boundaries.

SEASONAL CYCLE

Mixed-layer salinity shows a strong seasonal cycle. As Figure 4 indicates, the sum of the contributions (gray line) to salinity change from air-sea freshwater flux, ocean advection-diffusion, and entrainment well captures the annual evolution of the salinity tendency (black line) on the domain average, although the sum of the contributions has a slightly stronger amplitude when compared to the salinity

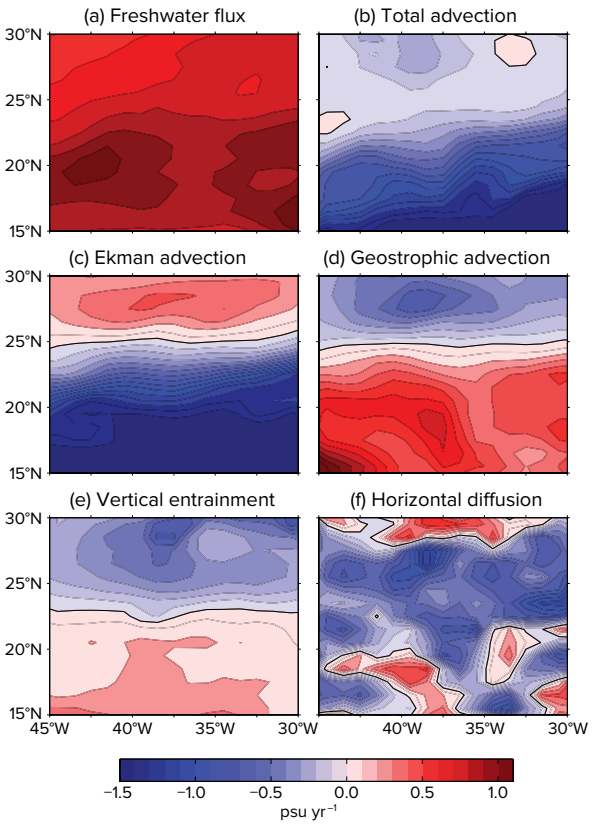

Figure 3. Time-mean (a) freshwater flux term, (b) oceanic advection, (c) Ekman advection, (d) geostrophic advection, (e) vertical entrainment, and (f) horizontal diffusion in SPURS-1 region. Units are psu yr^{-1}.

tendency. The sum of the forcing terms explains more than 90% of the variance in the salinity tendency. The salinity tendency is positive from April to August and negative from October to March, indicating that salinity in the mixed layer increases from spring to summer and decreases from fall to winter. The salinity tendency reaches its maximum in June and minimum in December.

The surface freshwater flux term dominates the mixed-layer salinity seasonal cycle (Figure 4a). This is different from results of Qu et al. (2011), who found that the oceanic processes explain half of the seasonal changes in the mixed-layer salinity tendency over the salinity maximum region (20°N–30°N, 24°W–52°W). The different results are likely due to the differences in study regions. Although evaporation dominates the time-mean freshwater flux in the SPURS-1 region, precipitation plays a slightly larger role in the seasonal variations of the surface freshwater flux. In addition, the mixed-layer depth also plays a role in the freshwater flux contribution to the seasonal evolution of the mixed-layer salinity (Figure 4b). The summertime E–P is close to its mean value, but the freshwater flux term ($(E–P)S_m/h_m$) has its maximum effect on increasing the mixed-layer salinity due to the shallow mixed layer, whereas during winter, when E–P reaches its maximum, the freshwater flux term is close to its minimum because of the deep wintertime mixed layer.

Although the surface freshwater flux term controls the seasonal evolution of mixed-layer salinity, there is a phase difference between the starting time of the salinity increase and that of the positive freshwater flux term, as well as the starting time of the freshening in the mixed layer and that of the negative freshwater flux term. For example, mixed-layer salinity starts to decrease in September, but the freshwater flux term does not fall below its mean value until October. This shift is due to the entrainment of fresher water from below as the mixed layer deepens. The entrainment reaches its maximum in May and minimum in December. Fresher water is entrained from the subsurface during fall/winter north of 23°N, which is somewhat compensated by saltier water entrained south of 23°N.

The oceanic advection and diffusion terms do not show a statistically significant seasonal cycle averaged over the entire region. Dividing the domain into two regions north and south of 25°N, we found that there is significant seasonality in the advection term in both regions, but they are out of phase (not shown). The seasonal variations in the advection term both north and south of 25°N are dominated by the Ekman component, with minimal contributions from the geostrophic component.

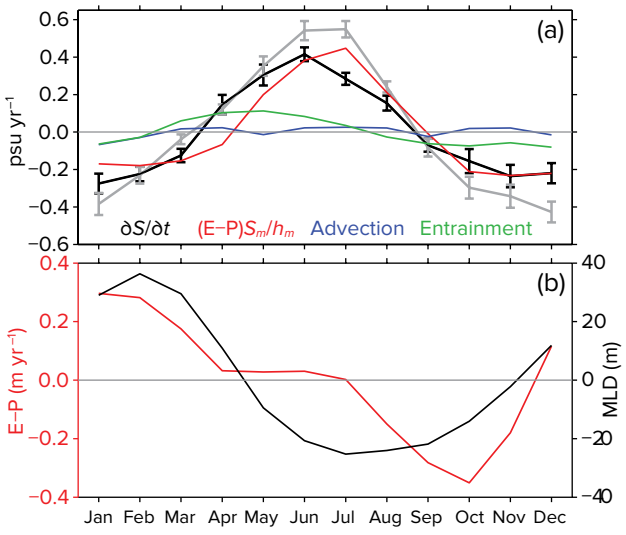

Figure 4. (a) Seasonal variations of the spatially averaged salinity tendency (black) and salinity budget terms in the SPURS-1 region: freshwater flux term (red), oceanic advection (blue), vertical entrainment (green), and the sum of these three terms (gray). The standard errors for the salinity tendency and the sum of the contributions are shown as vertical bars. (b) Freshwater flux, evaporation minus precipitation (E–P; red, left axis, and mixed-layer depth (black, right axis).

INTERANNUAL VARIATIONS

On interannual time scales, the domain-averaged salinity tendency fluctuates within ±0.1 psu yr^{-1} (Figure 5). Fluctuations in the salinity tendency exhibit an approximately four-year period, with positive anomalies during 2006–2007 and 2010–2011, and negative anomalies during 2004–2005, 2008–2009, and 2012–2013. Similar to the seasonal variations, the interannual variations in the mixed-layer salinity are well captured by the sum of the contributions to salinity change from air-sea freshwater flux, oceanic advection, diffusion, and entrainment. About 75% of the variance in the salinity tendency is captured by the sum of the forcing terms. However, unlike the freshwater flux dominance of seasonal variations, both the surface freshwater flux term and oceanic processes play important roles in interannual variations of mixed-layer salinity. The freshwater flux term shows positive anomalies between mid-2006 and mid-2010 and negative anomalies before mid-2006 and after mid-2010. Advection displays a decreasing trend during the study period, which is compensated by the increasing trend in the vertical entrainment and freshwater flux terms. Advection plays a larger role in salinity changes during 2008–2012, whereas the surface freshwater flux term dominates the surface salinity evolution during 2004–2007 and in 2013.

Interannual variations in the freshwater flux term mainly result from changes in precipitation, with minimal contributions from evaporation and mixed-layer depth changes. This is different from seasonal variations in the freshwater flux term where all three variables—evaporation, precipitation, and mixed-layer depth—play important roles. By dividing the advection term into geostrophic and Ekman components, we find that the contribution of the geostrophic advection is negligible; interannual variations in the advection term are dominated by the Ekman component (Figure 5c). As expected with strong meridional velocity and salinity gradients,

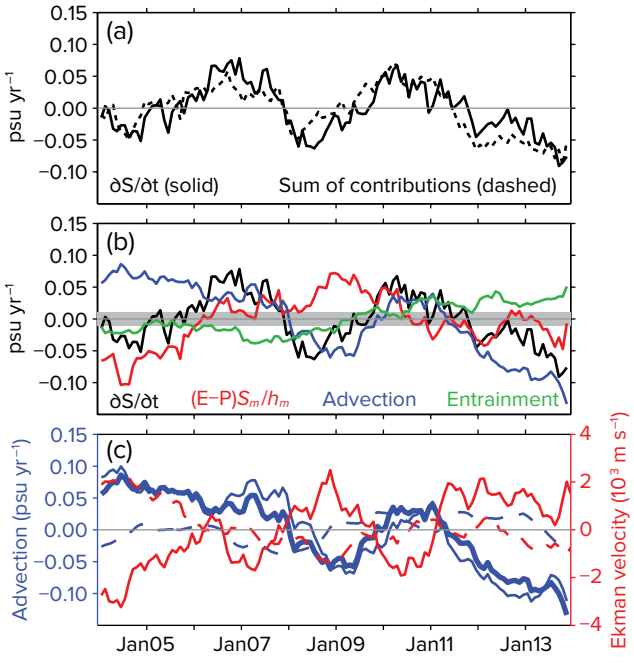

Figure 5. (a) Interannual variations of the spatially averaged salinity tendency (black) and the sum of the contributions from surface freshwater flux and oceanic processes (dashed). (b) Similar to (a), but with contributions from the freshwater flux term (red), oceanic advection (blue), and vertical entrainment (green) in the SPURS-1 region. The gray shading denotes the range where anomalies are not significantly different from zero. (c) Total advection term (thick blue) and its contributions from the Ekman (thin blue) and geostrophic (dashed blue) components, and the Ekman zonal (dashed red) and meridional (solid red) velocities.

changes in the Ekman advection term are largely controlled by the meridional component. Changes in both the meridional Ekman velocity and meridional salinity gradient contribute to the variations of the Ekman advection term. But, changes in the meridional Ekman velocity (Figure 5c, red line) due to changes in zonal wind stress play a larger role, explaining about 70% of the variance in the Ekman advection. Interannual variations in the vertical entrainment term are mainly due to changes in salinity differences between the mixed layer and just below the mixed layer. The salinities in the mixed layer and just below the mixed layer are highly correlated on interannual time scales, with a correlation coefficient of 0.95, well exceeding the 95% significance level of 0.18. However, changes in the mixed layer are relatively stronger than those in the subsurface. As a result, the interannual variations in the salinity difference are also highly correlated with the mixed-layer salinity itself.

LARGE-SCALE OCEAN CIRCULATION

There is no doubt that the dedicated SPURS-1 research effort will greatly improve our understanding of the processes governing upper-ocean salinity evolution in the subtropical North Atlantic. However, we should keep in mind that the role these processes play may vary during other periods. Our examination of the 10-year salinity changes indicates that surface salinity was relatively low during the period of the SPURS-1 field program. Although the surface freshwater flux term and oceanic advection often tend to compensate each other, they both contribute to the low salinity observed during the SPURS-1 period. The relationship between the freshwater flux term and oceanic advection is related to the spatial structure of the freshwater flux anomalies. During SPURS-1, the freshwater flux term induced large negative anomalies in salinity in the southeast of the region (Figure 6a, region enclosed by white ellipse), which was advected into the SPURS-1 region by the Ekman transport, strengthening the freshening effect of the freshwater flux. However, during 2004–2005 when the freshwater flux term also displayed negative anomalies, the anomalies were more focused in the western part of the region (Figure 6b), particularly to the northwest. In contrast, the freshwater flux in the southeast region (enclosed by white ellipse) resulted in positive anomalies in salinity. These positive anomalies were advected into the SPURS-1 region by the Ekman transport, which increased salinity in the SPURS-1 region, compensating the freshening effect from the freshwater flux. Therefore, it is important to understand large-scale forcing changes in order to understand surface salinity changes in the SPURS-1 region.

During SPURS-1, SSH anomalies were consistently higher than the long-term altimetry average (Figure 7a), a pattern that is persistent since approximately 2001. The altimetry SSH and surface drifter measurements are also used to examine eddy activity in the SPURS region. Despite discrepancies between the two measurements, both show that

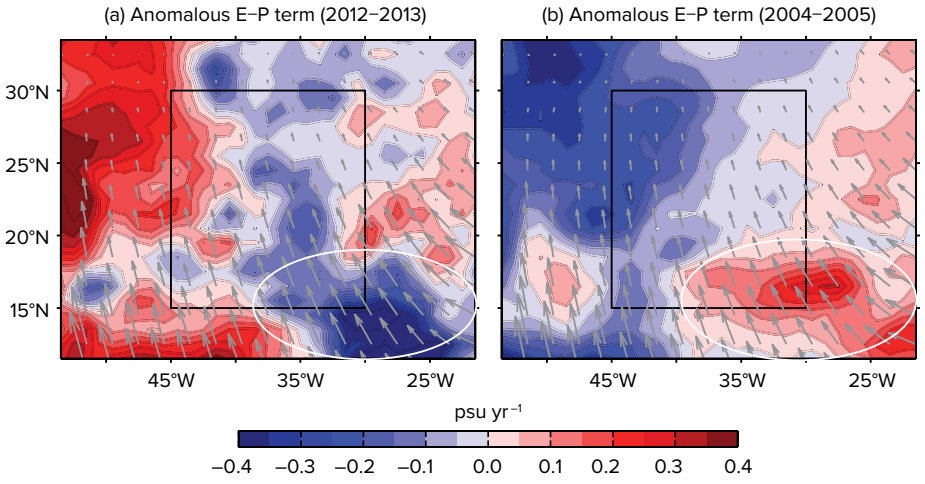

Figure 6. Anomalies of the freshwater flux term during (a) the SPURS-1 period of 2012–2013, and (b) during the years 2004–2005. Note the anomalies corresponding to salinity change due to freshwater flux forcing. Black boxes denote the SPURS region. Gray vectors show the Ekman velocity.

eddy kinetic energy (EKE) was relatively low during the SPURS-1 period (Figure 7), suggesting that lateral mixing may have had a stronger effect prior to the this time. Interestingly, our analysis of the EKE from altimetry and the residuals of the salinity budget on interannual time scales indicates that they are significantly anticorrelated, with a correlation coefficient of –0.56, exceeding the 95% significance level of 0.18. This suggests that the residual in the interannual salinity budget can be partly explained by unresolved mixing processes. Stronger mixing (positive EKE anomaly) would result in a negative residual, and weaker mixing (negative EKE anomaly) would result in a positive residual.

Sustained XBT measurements of temperature in the North Atlantic (Figure 8) also show strong interannual variations in subsurface temperatures. Compared to the historical record, the SPURS-1 region exhibits colder temperatures to the north of the region (AX07) and warmer temperatures in the southwestern region (AX08). Further examination of the subtropical gyre system using the altimeter data and the XBT measurements along the AX10 and AX08 transects demonstrates that the Gulf Stream, the western boundary current of the North Atlantic, was relative weak and had a more southerly position during 2012–2013. Although detailed studies are needed to understand how changes of the subtropical gyre system influence salinity changes in the SPURS-1 region, our statistical analysis of the Argo data suggests a significant anticorrelation of the salinity changes between the two regions on interannual time scales, with changes in the subtropical gyre region (25°N–40°N, 80°W–50°W) leading the SPURS-1 region by five months.

CONCLUSIONS

Our results from analysis of 10 years of salinity variations and contributions from the surface freshwater flux and oceanic processes suggest that the surface freshwater flux term strongly dominates the seasonal evolution of surface salinity in the SPURS-1 region of the North Atlantic, with vertical entrainment playing a secondary role. Although ocean advection plays a critical role in countering salinity increases from the surface freshwater flux term over the longer term, it does not show a significant seasonal cycle. The weak seasonality in ocean advection is due to out-of-phase seasonal variations in the regions north and south of the salinity maximum (25°N); however, oceanic advection plays an important role in interannual variations in surface salinity. The Ekman component dominates the interannual variations in the ocean advection term; contributions from the geostrophic advection term are negligible. Similar to the time-mean balance, ocean advection tends to compensate the surface freshwater flux effect on the interannual time scale, although both contribute to the low salinity during the SPURS-1 period. The exact role of ocean advection in surface salinity changes in the SPURS-1 region is related to the spatial distribution of the anomalous freshwater flux, suggesting the importance of large-scale forcing conditions. These results also indicate that sustained ocean observations are critical for placing short-term process studies in their long-term climatological context.

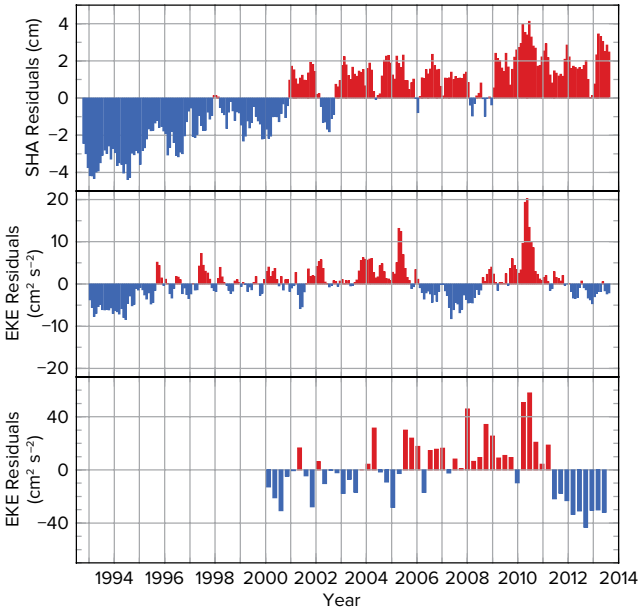

Figure 7. Sea surface height anomalies (SHA, top panel) and eddy kinetic energy (EKE) from altimetry (middle panel) and from surface drifters (bottom panel) averaged in the SPURS-1 region (15°N–30°N, 30°W–45°W). Units are cm for SHA and $cm^2\ s^{-2}$ for EKE.

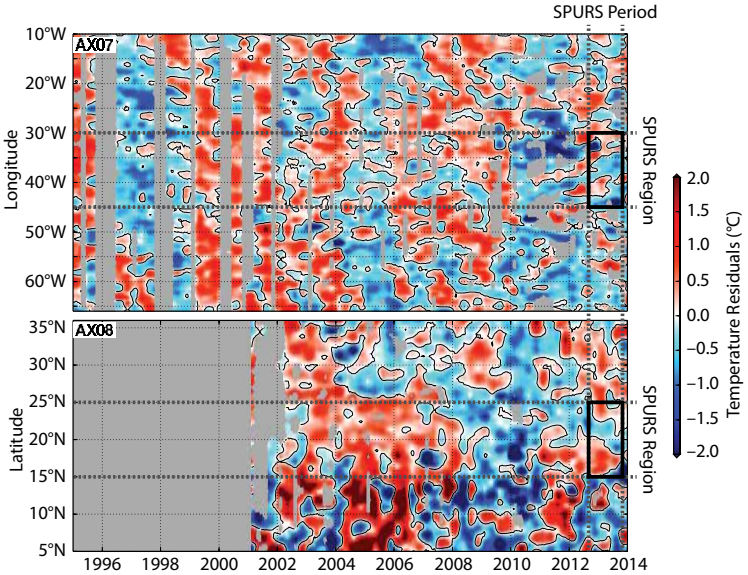

Figure 8. Hovmoller diagram of subsurface temperature anomalies at 100 m depth from XBT transects AX07 (top panel) and AX08 (bottom panel). Black boxes indicate the SPURS-1 period/region.

ACKNOWLEDGMENTS. The authors thank the two anonymous reviewers for their insightful comments. The authors would also like to thank Francis Bringas, Ricardo Domingues, and Joaquin Trinanes for their help in generating figures based on the sustained ocean observing system. This work was supported by NASA Grant NNX14AI85G, CIMAS Cooperative Agreement #NA10OAR4320143, and by NOAA/AOML. In situ data (Argo, XBT, surface drifters) used here correspond to the sustained ocean observing system, which is partly funded by the NOAA Climate Program Office. Surface drifter data can be found at http://www.aoml.noaa.gov/phod/dac/dacdata.php. XBT data are from http://www.aoml.noaa.gov/phod/hdenxbt/index.php.

REFERENCES

Adler, R.F., G.J. Huffman, A. Chang, R. Ferraro, P.-P. Xie, J. Janowiak, B. Rudolf, U. Schneider, S. Curtis, D. Bolvin, and others. 2003. The version-2 global precipitation climatology project (GPCP) monthly precipitation analysis (1979–present). *Journal of Hydrometeorology* 4:1,147–1,167, http://dx.doi.org/10.1175/1525-7541(2003)004<1147:TVGPCP>2.0.CO;2.

Bindoff, N.L., and T.J. McDougall. 2000. Decadal changes along an Indian Ocean section at 32°S and their interpretation. *Journal of Physical Oceanography* 30:1,207–1,222, http://dx.doi.org/10.1175/1520-0485(2000)030<1207:DCAAIO>2.0.CO;2.

Bingham, F.M., and R. Lukas. 1996. Seasonal cycles of temperature, salinity and dissolved oxygen observed in the Hawaii Ocean Time-series. *Deep Sea Research Part II* 43:199–213, http://dx.doi.org/10.1016/0967-0645(95)00090-9.

Bingham, F.M., G.R. Foltz, and M.J. McPhaden. 2012. Characteristics of the seasonal cycle of surface layer salinity in the global ocean. *Ocean Science* 8:915–929, http://dx.doi.org/10.5194/os-8-915-2012.

Boyer, T.P., and S. Levitus. 2002. Harmonic analysis of climatological sea surface salinity. *Journal of Geophysical Research* 107:1–14, http://dx.doi.org/10.1029/2001JC000829.

Broecker, W.S. 1997. Thermohaline circulation, the Achilles heel of our climate system: Will man-made CO_2 upset the current balance? *Science* 278:1,582–1,588, http://dx.doi.org/10.1126/science.278.5343.1582.

Curry, R., and C. Mauritzen. 2005. Dilution of the northern North Atlantic Ocean in recent decades. *Science* 308:1,772–1,774, http://dx.doi.org/10.1126/science.1109477.

Curry, R., B. Dickson, and I. Yashayaev. 2003. A change in freshwater balance of the Atlantic Ocean over the past four decades. *Nature* 426:826–829, http://dx.doi.org/10.1038/nature02206.

de Boyer Montégut, C., G. Madec, A.S. Fischer, A. Lazar, and D. Iudicone. 2004. Mixed layer depth over the global ocean: An examination of profile data and a profile-based climatology. *Journal of Geophysical Research* 109, C12003, http://dx.doi.org/10.1029/2004JC002378.

de Boyer Montégut, C., J. Mignot, A. Lazar, and S. Cravatte. 2007. Control of salinity on the mixed layer depth in the world ocean: Part 1. General description. *Journal of Geophysical Research* 112, C06011, http://dx.doi.org/10.1029/2006JC003953.

Dee, D.P., S.M. Uppala, A.J. Simmons, P. Berrisford, P. Pali, S. Kobayshi, U. Andrae, M.A. Balmaseda, G. Balsamo, P. Bauer, and others. 2011. The ERA-Interim reanalysis: Configuration and performance of the data assimilation system. *Quarterly Journal of the Royal Meteorological Society* 137:553–597, http://dx.doi.org/10.1002/qj.828.

Dong, S., S.L. Garzoli, and M.O. Baringer. 2009. An assessment of the seasonal mixed-layer salinity budget in the Southern Ocean. *Journal of Geophysical Research* 114, C12001, http://dx.doi.org/10.1029/2008JC005258.

Ducet, N., P.-Y. Le Traon, and G. Reverdin. 2000. Global high resolution mapping of ocean circulation from TOPEX/POSEIDON and ERS-1 and -2. *Journal of Geophysical Research* 105:19,477–19,498, http://dx.doi.org/10.1029/2000JC900063.

Durack, P.J., and S.E. Wijffels. 2010. Fifty-year trends in global ocean salinities and their relationship to broad-scale warming. *Journal of Climate* 23:4,342–4,362, http://dx.doi.org/10.1175/2010JCLI3377.1.

Durack, P.J., S.E. Wijffels, and R.J. Matear. 2012. Ocean salinities reveal strong global water cycle intensification during 1950 to 2000. *Science* 336:455–458, http://dx.doi.org/10.1126/science.1212222.

Fedorov, A.V., R.C. Pacanowski, S.G. Philander, and G. Boccaletti. 2004. The effect of salinity on the wind-driven circulation and the thermal structure of the upper ocean. *Journal of Physical Oceanography* 34:1,949–1,966, http://dx.doi.org/10.1175/1520-0485(2004)034<1949:TEOSOT>2.0.CO;2.

Foltz, G.R., and M.J. McPhaden. 2008. Seasonal mixed layer salinity balance of the tropical North Atlantic Ocean. *Journal of Geophysical Research* 113, C02013, http://dx.doi.org/10.1029/2007JC004178.

Godfrey, J.S., E.F. Bradley, P.A. Coppin, L.F. Pender, T.J. McDougall, E.W. Schulz, and I. Helmond. 1999. Measurements of upper ocean heat and freshwater budgets near a drifting buoy in the equatorial Indian Ocean. *Journal of Geophysical Research* 104:13,269–13,302, http://dx.doi.org/10.1029/1999JC900045.

Gregory, J.M., K.W. Dixon, R.J. Stouffer, A.J. Weaver, E. Driesschaert, M. Eby, T. Fichefet, H. Hasumi, A. Hu, J.H. Jungclaus, and others. 2005. A model intercomparison of changes in the Atlantic thermohaline circulation in response to increasing atmospheric CO_2 concentration. *Geophysical Research Letters* 32, L12703, http://dx.doi.org/10.1029/2005GL023209.

Häkkinen, S. 1999. Variability of the simulated meridional heat transport in the North Atlantic for the period 1951–1993. *Journal of Geophysical Research* 104:10,991–11,007, http://dx.doi.org/10.1029/1999JC900034.

Huang, B., V.M. Mehta, and N. Schneider. 2005. Oceanic response to idealized net atmospheric freshwater in the Pacific at the decadal time scale. *Journal of Physical Oceanography* 35:2,467–2,486, http://dx.doi.org/10.1175/JPO2820.1.

Johnson, E.S., G.S.E. Lagerloef, J.T. Gunn, and F. Bonjean. 2002. Surface salinity advection in the tropical oceans compared with atmospheric freshwater forcing: A trial balance. *Journal of Geophysical Research* 107(C12), 8014, http://dx.doi.org/10.1029/2001JC001122.

Josey, S.A., and R. Marsh. 2005. Surface freshwater flux variability and recent freshening of the North Atlantic in the eastern subpolar gyre. *Journal of Geophysical Research* 110, C05008, http://dx.doi.org/10.1029/2004JC002521.

Lukas, R., and E. Lindstrom. 1991. The mixed layer of the western equatorial Pacific Ocean. *Journal of Geophysical Research* 96:3,343–3,357, http://dx.doi.org/10.1029/90JC01951.

O'Connor, B.M., R.A. Fine, and D.B. Olson. 2005. A global comparison of subtropical underwater formation rates. *Deep Sea Research Part I* 52:1,569-1,590, http://dx.doi.org/10.1016/j.dsr.2005.01.011.

Qu, T., S. Gao, and I. Fukumori. 2011. What governs the North Atlantic salinity maximum in a global GCM? *Geophysical Research Letters* 38, L07602, http://dx.doi.org/10.1029/2011GL046757.

Qu, T., S. Gao, and I. Fukumori. 2013. Formation of salinity maximum water and its contribution to the overturning circulation in the North Atlantic as revealed by a global general circulation model. *Journal of Geophysical Research* 118:1,982–1,994, http://dx.doi.org/10.1002/jgrc.20152.

Rahmstorf, S. 1995. Multiple convection patterns and thermohaline flow in an idealized OGCM. *Journal of Climate* 8:3,028–3,039, http://dx.doi.org/10.1175/1520-0442(1995)008<3028:MCPATF>2.0.CO;2.

Roemmich, D., and J. Gilson. 2009. The 2004–2008 mean and annual cycle of temperature, salinity, and steric height in the global ocean from the Argo program. *Progress in Oceanography* 82:81–100, http://dx.doi.org/10.1016/j.pocean.2009.03.004.

Schmitt, R.W. 2008. Salinity and the global water cycle. *Oceanography* 21(1):12–19, http://dx.doi.org/10.5670/oceanog.2008.63.

Schmitt, R.W., and A.Blair. 2015. A river of salt. *Oceanography* 28(1):40–45, http://dx.doi.org/10.5670/oceanog.2015.04.

Sprintall, J., and M. Tomczak. 1992. Evidence of the barrier layer in the surface layer of the tropics. *Journal of Geophysical Research* 97:7,305–7,316, http://dx.doi.org/10.1029/92JC00407.

Stocker, T.F., and A. Schmittner. 1997. Influence of CO_2 emission rates on the stability of the thermohaline circulation. *Nature* 388:862–865.

Vinogradova, N.T., and R.M. Ponte. 2013. Clarifying the link between surface salinity and freshwater fluxes on monthly to interannual time scales, *Journal of Geophysical Research* 118:3,190–3,201, http://dx.doi.org/10.1002/jgrc.20200.

Wong, A., N.L. Bindoff, and J.A. Church. 1999. Large-scale freshening of intermediate waters in the Pacific and Indian Oceans. *Nature* 400:440–443, http://dx.doi.org/10.1038/22733.

Yu, L. 2011. A global relationship between the water cycle and near-surface salinity. *Journal of Geophysical Research* 116, C10025, http://dx.doi.org/10.1029/2010JC006937.

Yu, L., and R.A. Weller. 2007. Objectively analyzed air-sea heat fluxes for the global ice-free oceans (1981–2005). *Bulletin of the American Meteorological Association* 88:527–539, http://dx.doi.org/10.1175/BAMS-88-4-527.

AUTHORS. **Shenfu Dong** (shenfu.dong@noaa.gov) is Associate Scientist, Cooperative Institute for Marine and Atmospheric Studies, University of Miami, and National Oceanic and Atmospheric Administration, Atlantic Oceanographic and Meteorological Laboratory (NOAA/AOML), Miami, FL, USA. **Gustavo Goni** is Physical Oceanographer, and **Rick Lumpkin** is Oceanographer, both at NOAA/AOML, Miami, FL, USA.

ARTICLE CITATION

Dong, S., G. Goni, and R. Lumpkin. 2015. Mixed-layer salinity budget in the SPURS region on seasonal to interannual time scales. *Oceanography* 28(1):78–85, http://dx.doi.org/10.5670/oceanog.2015.05.